GLASS/EPOXY POLYMER NANOCOMPOSITES: MANUFACTURING AND MECHANICAL PROPERTIES

A
Thesis Report

Submitted in partial fulfilment of the requirement for the award of degree

MASTER OF ENGINEERING
in
CAD/CAM & ROBOTICS

Submitted By
Dawinder Singh
(Roll No. 801081008)

Under Guidance of

Mr. BIKRAMJIT SHARMA
Assistant Professor
Deptt. Of Mechanical Engg.
Thapar University, Patiala

Dr. RAJEEV MEHTA
H.O.D & Associate Professor
Deptt. Of Chemical Engg.
Thapar University, Patiala

MECHANICAL ENGINEERING DEPARTMENT

THAPAR UNIVERSITY, PATIALA-147004, INDIA

July 2012

CERTIFICATE

This is to certify that the work in this thesis report entitled **"GLASS/EPOXY POLYMER NANOCOMPOSITES: MANUFACTURING AND MECHANIAL PROPERTIES"** submitted in partial fulfilment of requirement for the award of **Master of Engineering Degree in CAD/CAM & Robotics** in Mechanical Department of Thapar University, Patiala, is an authentic record of work carried out by me under the guidance of **Mr. Bikramjit Sharma**, Assistant Professor, Mechanical Engineering Department, Thapar University, Patiala and **Dr. Rajeev Mehta**, H.O.D. & Associate Professor, Chemical Engineering Department, Thapar University, Patiala.

The matter embodied in this report has not been submitted in part or full to any university or institute for the award of any degree.

Dawinder Singh

Dawinder Singh

Dated: 15/7/12

This is to certify that the above declaration made by the student concern is correct to the best of my knowledge and belief.

Mr. Bikramjit Sharma
Assistant Professor
Deptt. Of Mechanical Engg.
Thapar University, Patiala.

Dr. Rajeev Mehta
H.O.D & Associate Professor
Deptt. Of Chemical Engg.
Thapar University, Patiala.

Countersigned By:

Dr. Ajay Batish
Professor & Head M.E.D
Thapar University, Patiala.

Dr. S. K. Mohapatra
Dean Academics Affairs
Thapar University, Patiala.

ACKNOWLEDGEMENT

I am highly grateful to the authorities of Thapar University, Patiala for providing this opportunity to carry out the Thesis work.

I would like to express a deep sense of gratitude and thank profusely my thesis guide **Mr. Bikramjit Sharma**, Assistant Professor, Mechanical Engineering Department, Thapar University, Patiala and **Dr. Rajeev Mehta**, H.O.D. & Associate Professor, Chemical Engineering Department, Thapar University, Patiala for their sincere & invaluable guidance, suggestions and attitude which inspired me to submit report in the present form.

I am highly thankful to **Mr. Toyesh** (Ph.D Scholar in Chemical Engineering Department) for his invaluable guidance & continuous support.

I am also thankful to other faculty members and all the workshop staff of Mechanical Department, Thapar University, Patiala and Chemical Engineering Department, Thapar University, Patiala for their support.

I would also like to thank and acknowledge **BASF Construction Chemicals (India) Private Limited and Connell Bros. Mumbai** for supplying us generously with E-Glass Fibre sheet, M Brace epoxy (Base and hardener) and Clay (Closite 30B®) etc. for this experimentation.

My special thanks are due to my family members and friends who constantly encouraged me to complete this study.

Dawinder Singh

DAWINDER SINGH

ABSTRACT

Nanotechnology involves the control and manipulation of materials at the nanoscale. As the surface area of a particle increases, creating more sites for bonding, catalysis or reaction with surrounding materials, resulting in improved properties such as increased strength or chemical or heat resistance. In the present work, epoxy modified with nanoclay cloisite 30B (having concentration 0.5wt%, 2wt%, 3wt% and 4wt% of epoxy) is reinforced with C-glass chopped strand fiber and E-glass unidirectional fiber to manufacture interply laminates. X-ray diffraction conducted on epoxy clay nanocomposites indicates exfoliation of nanoclay at all level of nanoclay loading. The effect of varying the nanoclay concentration is observed by carrying out tensile, 3-point bending strength test and hardness tests. Test result shows that tensile strength increases as the clay concentration varies from 0wt% to 3wt%. Tensile strength is maximum at 3wt% and further increase in clay concentration shows decrease in tensile strength. Flexural strength increases as the clay concentration varies from 0wt% to 4wt%. Micro hardness increases as clay concentration varies from 0wt% to 2wt% and then decrease at further loading. Further hygrothermal studies on nanocomposites have been performed in water and NaOH baths. During exposure it is observed that the properties degradation in NaOH is more as compared to water.

TABLE OF CONTENT

LIST OF FIGURES

LIST OF TABLES

NOMENCLATURE AND ABBREVATIONS

GFRP	glass fiber reinforced polymer
VLSI	very large scale integration
PNC	polymer nanocomposites
OMMT	monomorillonite organoclay
CNF's	carbon nanofibers
CNT's	carbon nanotubes
WXRD	wide angle x-ray diffraction
PAN	polyacrylonitrile
SEM	scanning electron microscope
CTE	coefficient of thermal expansion
CAI	compression after impact

CHAPTER 1 INTRODUCTION

Nanotechnology involves the control and manipulation of materials at the nanoscale (particle sizes from 1 to 100 nanometre (nm), where 1 nm equals 1 billionth of a meter) to create new materials and structures that have novel properties due to their small size (increased surface area). Materials with dimensions on the nanometres scale (10^{-9}meter) often have properties dramatically different from their bulk-scale counterparts [Sakaki, 1994]. At nanolevel, some compounds transform from electrical insulator to conductors, from fragile to tough. One of the major factors, which alter these properties, is the increase in the ratio of surface area to volume. As the surface area of a particle increases, creating more sites for bonding, catalysis or reaction with surrounding materials, resulting in improved properties such as increased strength or chemical or heat resistance. Hence, due to the high surface-to volume ratio associated with nanometre sized particles it is possible to control the fundamental properties of materials through the surface/size effect. There is a great variety of nanomaterials and their range of properties and possible applications appears to be enormous, from extra-ordinary tiny electronics devices, including miniature batteries, to biomedical uses and as components of parts of automobiles.

Nanotechnology is directed towards the formation of various nanomaterials such as:

- Nanocomposites
- Nanofiber
- Nanoparticulate fillers
- Nanoporous

1.1 Nanocomposites

A nanocomposite is as a multiphase solid material where one of the phases has one, two or three dimensions of less than 100 nanometer (nm), or structures having nano-scale repeat distances between the different phases that make up the material. In the broadest sense this definition can include porous media, colloids, gels and copolymer. The mechanical, electrical, thermal, optical, electrochemical, catalytic properties of the nano-composite will differ markedly from that of the component materials.

Nanocomposites are found in nature, for example in the structure of the abalone shell and bone. The use of nanoparticle-rich materials long predates the understanding of the physical and chemical nature of these materials. Jose-Yacaman *et al.* (1996) investigated the origin of the depth of color and the resistance to acids and bio-corrosion of maya blue paint, attributing it to a nanoparticle mechanism. From the mid 1950s nanoscale organo-clays have been used to control flow of polymer solutions (e.g. as paint viscosifiers) or the constitution of gels (e.g. as a thickening substance in cosmetics, keeping the preparations in homogeneous form). By the 1970s polymer/nano composites were the topic of textbooks, although the term "nanocomposites" was not in common use.

In mechanical terms, nanocomposites differ from conventional composites due to the exceptionally high surface to volume ratio of the reinforcing phase and/or its exceptionally high aspect ratio. The reinforcing material can be made up of particles (e.g. minerals), sheets (e.g. exfoliated clay stacks) or fibers (e.g. carbon nanotubes or electrospun fibers). The area of the interface between the matrix and reinforcement phase(s) is typically an order of magnitude greater than for conventional composite materials. The matrix material properties are significantly affected in the vicinity of the reinforcement. Ajayan *et al.* (1992) found that with polymer nanocomposites, properties related to local chemistry, degree of thermoset cure, polymer chain mobility, polymer chain conformation, degree of polymer chain ordering or crystallinity can all vary significantly and continuously from the interface with the reinforcement into the bulk of the matrix.

This large amount of reinforcement surface area means that a relatively small amount of nanoscale reinforcement can have an observable effect on the macroscale properties of the composite. For example, adding carbon nanotubes improves the electrical and thermal

conductivity. Other kinds of nanoparticulates may result in enhanced optical properties, dielectric properties, heat resistance or mechanical properties such as stiffness, strength and resistance to wear and damage. In general, the nano reinforcement is dispersed into the matrix during processing. The percentage by weight (called *mass fraction*) of the nanoparticulates introduced can remain very low (on the order of 0.5% to 5%) due to the low filler prelocation, threshold especially for the most commonly used non-spherical, high aspect ratio fillers (e.g. nanometer-thin platelets, such as clays, or nanometer-diameter cylinders, such as carbon nanotubes).

1.2 Polymer nanocomposites

For many fields of the modern industry appreciable improvement of physicomechanical properties of polymeric materials. Now a days, the most perspective decision of this problem is a modified polymer with nanostructure fillers – creation of polymeric nanocomposites.

Polymer nanocomposites (PNC) are polymers (thermoplastics, thermosets, elastomers) that have been reinforced with small quantities (less than 5% by weight) of nano-sized particles. Uniform dispersion of nanoparticles in polymer matrix produces ultra- large interfacial area per volume between the nanoparticle and the host polymer. This immense internal interfacial area and the nanoscopic dimension between nanoparticles fundamentally differentiate PNCs from traditional composites and filled plastics.

Introduction to nanoparticles to polymer matrix ensure significant property improvements with very low loading levels. Traditional micro particles additives require much higher filler concentration to achieve similar results. The most commonly used nano fillers are:

1. Manomorillonite organoclays (OMMT)
2. Carbon nanofibers (CNFs)
3. Carbon nanotubes (CNTs)
4. Metallic nanoparticles

The value of PNC technology comes from providing value added properties not present in the neat polymer, without sacrificing the inherent processibility and mechanical properties of the polymer. Some of the major advantages of the polymer nanocomposites are:

Mechanical Properties:

- High adhesion of nanoparticles to polymer matrix results in the enhanced strength of nanocomposites relative to conventional composite.
- Small size of nanoparticles ensures small size of pores in the case of exfoliation of a matrix from filler particles. It results in the strength increase too.
- Introduction of small amount of nanoparticles to polymer significantly enhance the adhesion of polymer to different substance.

Optical Properties:

- Nanocomposites are optically more transparent in comparison to conventional composites.
- Special optical effects.
- Optical clarity in comparison to conventionally filled polymers.

Magnetic Properties:

- In some case composites with magnetic nanoparticles have the magnetoresistance and magnetic permeability much higher than in the case of conventional composites.
- It is possible to make composites with magnetic threshold concentration smaller than electrical percolation threshold.

1.3 Epoxy nanocomposites

In 1946, the first industrially-produced epoxy resin was introduced to market. Since then, the use of thermosetting polymers has steadily increased. The wide range of epoxy resin applications includes: coating, electrical, automotive, marine, aerospace and civil infrastructure as well as tool fabrication and pipes and vessels in the chemical industry. Due to their low density of around 1.3 g/cm and good adhesive and mechanical properties, epoxy resin became a promising material for high performance applications in the transport industry, usually in the form of composite materials such as fiber composite or in honeycomb structures. In the aerospace industry, epoxy-composites material can be found in various part of the body and structure of military and civil aircrafts, with the number of applications on the rise. A recent

approach to improve and diversify polymer properties in the aerospace industries is through the dispersion of nanometer-scaled fillers in the polymer matrix. [Njuguna and Pielichowski, 2003]. A significant number of academic and industrial projects have investigated the possibilities to further improve epoxy resin (and in some cases composites or other binary systems) through the strategy of producing nanocomposites.

The term 'epoxy resin' refers to both the polymer and its cured resin/hardener system. The former is a low molecular weight oligomer that contains one or more epoxy groups per molecule (more than one unit per molecule is required if the resultant material is to be cross-linked). The characteristic group, a three-member ring known as epoxy, epoxide, oxirane, glycidyl or ethoxyline group is highly strained and therefore very reactive. Epoxy resins can be cross-linked through a polymerization reaction with a hardener at room temperature or at elevated temperature (latent reaction). Curing agents used for room temperature cure are usually aliphatic amines, whilst commonly used higher temperature, higher performance hardener are aromatic amines and acid anhydrides. However, an increasing number of specialized curing agents, such as poly-functional amines, polybasic carboxylic acids, mercaptans and inorganic hardener are also used. All of these results in different, tailored properties of the final polymer matrix. In general, the higher temperature Cured resin systems have improved properties, such as higher glass transition temperatures, strength and stiffness, compared to those cured at room temperature.

1.4 Clay nanoparticles

Clay as nanoparticles such as smectic clays (e.g. montmorillonite) are incorporated into polymers to form resulting polymer nanocomposite, which may possess unique electrical, mechanical and optical properties.

As their name suggests, polymer/clay nanocomposites comprise organic/inorganic hybrid polymer matrices containing platelet-shaped clay particles that have sizes of the order of a few nanometers thick and several hundred nanometer long. Partly because of their aspect ratios and high surface areas, the clay particles, if properly dispersed in the polymer matrix at a loading level of 1wt% to 5 wt. % of polymer, impart unique combinations of physical and chemical properties that make these nanocomposites attractive for making films and coatings for a variety

of industrial applications. Relative to the unmodified polymer, the polymer clay nanocomposites may exhibit improvements in strength, modulus, and toughness, tear, radiation, fire resistance, and lower thermal expansion and permeability to gases while retaining a high degree of optical transparency [www.techbriefs.com].

The most common type of nanoclay is montmorillonite (MMT), a layered aluminosilicate in the smectite family of clay. Unlike clay minerals such as talc and mica that have been used as fillers for years, MMT can be delaminated and dispersed into an individual layers only one nanometer thick by about 70 nm to 150 nm across. The result is a radical increase in the surface area-to-volume ratio: with a surface area of 750 m^2/g, 20g of MMT platelets could cover a football field! Montmorillonite, can absorb 20-30 times its volume of water, and is of particular interest to the plastics industry. It is a 2:1 layered structured, a single layer of aluminum octahedra sandwiched between two layers of silicon tetrahedral. Each layered sheet is slightly less than one nanometer, with surface dimensions extending to about a micron (1,000 nanometers). With aspect ratios approaching 1,000, surface area of the clay is in the range of 750 m^2/g.

According to the structure three different types of clay-polymer composites can be distinguished. (Fig. 1.1) [Alexandre, 2000].

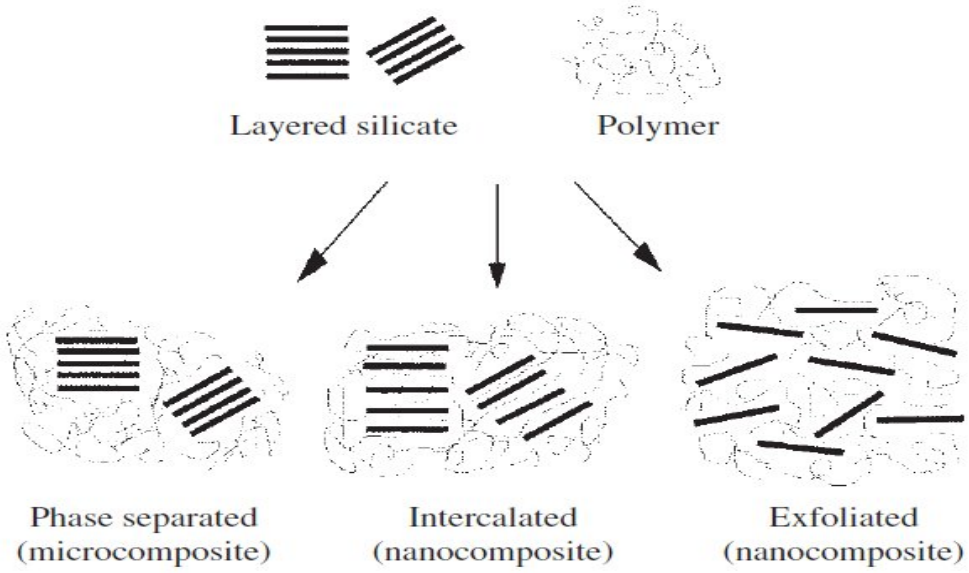

Fig. 1.1 Three idealized structures of polymer-clay composites[1]

- When the matrix polymer chains are unable to penetrate between the layers of the silicate particles a conventional composite is formed
- Intercalated structures are formed when one or more polymer chains intercalate between the layers. Hereby the interlayer spacing is increased but the ordered layer structure of the clay particles is retained as can be observed by wide angle X-ray diffraction (XRD).
- In exfoliated composites the clay particles are completely delaminated and the silicate layers do not show any periodicity in their arrangement.

Dispersing clay in the polymer is very difficult and therefore a compatibilizing agent is commonly used. Compatibilizing agent is a molecule constituted of one hydrophilic and one organophilic function. The compatibilizing agents allow dispersing layered silicates in polymers by substitutions of the metallic cations between the silicate layers

1.5 Introduction to fiber reinforced polymers (FRP)

Fiber-reinforced polymer is a composite material made of a polymer matrix reinforced with fibers. The fibers are usually fiber glass, carbon or aramid, while the polymer is usually an epoxy, vinyl ester or polyester thermosetting plastic. FRPs are commonly used in the aerospace,automotive, marine, and construction industries. The strength properties of FRP collectively make up one of the primary reasons for which civil engineers select them in the design structures. A material's strength is governed by its ability to sustain a load without excessive deformation or failure. When an FRP specimen is tested in axial tension, the applied force per unit cross-sectional area (stress) is proportional to the ratio of change in a specimen's length to its original length (strain). When the applied load is removed, FRP returns to its original shape or length. In other words, FRP responds linear-elastically to axial stress. The response of FRP to axial compression is reliant on the relative proportion in volume of fibres, the properties of the fibre and resin, and the interface bond strength. FRP's response to transverse tensile stress is very much dependent on the properties of the fiber and matrix, the interaction between the fiber and matrix, and the strength of the fiber-matrix interface. Generally tensile strength in this direction is very poor

1.6 Advantages of fiber reinforced polymers

- High strength to weight ratio.
- Corrosion resistant.
- Can be tailored for the application (both shape and type of FRP).
- Cost of installation time (both direct and indirect) is also low.
- Cost of installation versus replacement is low.
- FRP has a low cost considering other materials.

1.7 Types of fiber

1.7.1. Glass fiber: Glass fiber is a material made from extremely fine fibers of glass, and it is the largest reinforcement measured in sales. Glass fiber was invented in 1938 by Russell Games Slayter of Owens-Corning as a material to be used as insulation [Lowenstein, 1973]. Ever since then, glass fiber has become widely used as insulation and composite reinforcement material. Based on the composition and the application, glass fibers can be classified in several types.

Fig.1.2 Commercially available glass fibers [12]

The most commonly used glass fiber type for composite applications is E-glass, due to its relatively good mechanical properties and high electrical insulation. S-glass is also used in composite materials where high tensile strength is desired, however this material comes at a

much higher cost. R-glass is also used in composite materials with high mechanical requirements such as fatigue life and high chemical resistance. The typical fiber diameter for glass fiber is 9-17 μm and the specific gravity is about 2.5. The tensile strength of glass fiber is in the order of 2000-4800 MPa and the elastic modulus is in the order of 50-90 GPa, much higher than that of polymers [Biron, 1973].

Types of Glass Fibers:-

E-glass (electrical) - lower alkali content and stronger than A glass (alkali). Good tensile and compressive strength and stiffness, good electrical properties and relatively low cost, but impact resistance relatively poor. E-glass is the most common form of reinforcing fibre used in polymer matrix composites.

C-glass (chemical) - best resistance to chemical attack. Mainly used in the form of surface tissue in the outer layer of laminates used in chemical and water pipes and tanks.

R,S or T-glass- manufacturers trade names for equivalent fibres having higher tensile strength and modulus than E glass, with better wet strength retention. Higher Inter laminar shear strength and wet out properties are achieved through smaller filament diameter. Developed for aerospace and defense industries, and used in some hard ballistic armour applications. This factor, and low production volumes mean relatively high price.

1.7.2. Carbon fiber

Carbon fiber is another major fiber reinforcement type used in FRPC. One of the most common methods of manufacturing carbon fiber is the oxidation and thermal pyrolysis of polyacrylonitrile (PAN), so called PAN-based carbon fibers. This material consists of extremely thin fibers about 5-10 μm in diameter and comprised mostly of carbon atoms. The carbon atoms are bonded together in microscopic crystals that are mostly aligned parallel to the long axis of the fiber. This alignment makes the fiber show very high tensile properties. The tensile strength of carbon fiber is in the order of 3000-5800 MPa and the elastic modulus is in the order of 500-600 GPa [Lowenstein, 1973].

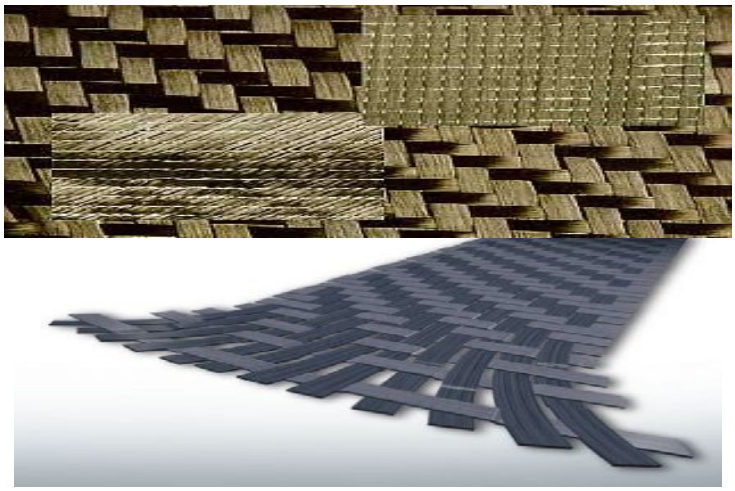

Fig. 1.3 Different types of matted carbon fibers [12]

Compared with glass fibers, carbon fibers have lower density but higher tensile strength and elastic modulus. These properties make carbon fiber an ideal reinforcement for composite materials used in aircraft components, high-performance vehicles, sporting equipment, wind generator blades, and other high demand, high performance applications.

1.8 Applications of glass fibre reinforced polymers

- Sailplanes, sports cars, body shells, boats, flat roofs, Lorries, wind turbine blades.
- Pods, domes and architectural features where a light weight is necessary.
- Bodies for automobiles.
- FRP tanks and vessels: FRP is used extensively to manufacture chemical equipments and tanks and vessels.
- UHF-broadcasting antennas are often mounted inside a glass-reinforced plastic cylinder on the pinnacle of a broadcasting tower.
- Engine intake manifolds are made from glass fiber reinforced PA 66

Wang *et al.* (2001) prepared polymeric nano-composites by melt intercalation method. The nanoclay was mixed with polymer by twin-screw extrusion. The clay-spacing in the composites was measured by X-ray diffraction (XRD). The morphology of the composites and its development during the extrusion process were observed by scanning electron microscopy **(**SEM**).** Melt viscosity and mechanical properties of the composites and the blends were also measured. It was found that the clay spacing in the composites was influenced greatly by the type of polymer used. Also the addition of the nanoclay increased the viscosity of the polymer when there was a strong interaction between the polymer and the nanoclay. The mechanical test showed that the addition of 5-10 wt.% nano-clay largely increased the elastic modulus of the composites. The water absorption of nylon 6 was decreased with the presence of nano-clay. The effect of nano-clay on polymers and polymer blends was also compared with Kaolin clay under the same experimental conditions.

Sinha Ray *et al.* (2003) discussed the academic and industrial aspects of the preparation, characterization, materials properties, crystallization behavior, melt rheology and processing of polymer/layered silicate nanocomposites. Smectites were a valuable mineral class for industrial applications because of their high cation exchange capacities, surface area, surface reactivity, adsorptive properties. These composites exhibited improved mechanical properties compared to conventional composites. The composites exhibited a remarkable increase in thermal stability, as well as self-extinguishing characteristics for flammability, such that the flammability of pristine polymers were significantly reduced after nanocomposite formation with layered silicate.

Chow *et al*. (2005) analysed the water absorption and hygrothermal aging behaviour of organomontmoiillonite (OMMT reinforced polyamide 6/polypropylene (PA6/PP ratio = 70/30), with and without maleated PP (MAH-g-PP), at three different temperatures (30, 60, and 90^{o}C. The water absorption of the PA6/PP nanocomposites obeyed the Fickian law behavior. It was found that the equilibrium moisture content and the diffusion coefficients were dependent on the OMMT loading, MAH-g-PP concentration and immersion temperature tensile modulus and strength of PA6/PP nanocomposites deteriorated after exposure to hygrothermal aging. Water acted as a plasticizer for the PA6/PP matrix and silicate layer of OMMT. The nanocomposites

showed excellent retention ability and recovery properties under any immersion temperature. The MAH-g-pp enhanced the resistance of the nanocomposites against water immersion and also improved the resistance against hygrothermal attack.

Kornmann *et al*. (2005) synthesized and successfully used epoxy-layered silicate nanocomposites based on anhydride cured epoxy and octadecylamine modified fluorohectorite as matrix in glass-fiber-reinforced laminates by hand lay-up technique. The material used was the synthetic layered silicate Somasif ME-100. One hundred and twenty milli-equivalents per 100 g of Somasif ME-100 of ocadecylamine were dispersed in deionised water at 80^{o}C. They had done the flexural tests on the laminates and indicated that the presence of silicate layers in the epoxy matrix leads to a flexural strength improvement of 27%. According to dynamic mechanical measurements, the presence of organosilicate caused a decrease of the glass transition temperature. The glass transition temperature decrease was apparently responsible for the larger water uptake observed in the nanocomposite.

Lin *et al*. (2005) prepared Layered silicate/glass fiber/epoxy hybrid composites using vacuum-assisted resin transfer molding (VARTM) process. Unidirectional glass fibers were placed in two directions: parallel and perpendicular to the resin flow direction. The intercalation behavior of the clay and the morphology of the composites were investigated using X-ray diffraction (XRD) and transmission electron microscopy (TEM). The complementary use XRD and TEM techniques revealed an intercalated clay structure in the composites. Dispersion of clay in the composites was also observed using scanning electron microscopy (SEM); The nanoclay were dispersed between both the bundles of glass fibers and within the interstices of the fiber filaments. The mechanical properties of the ternary composites were evaluated. The results indicated that introducing a small amount of organoclay to the glass fiber/epoxy composites enhanced their mechanical and thermal properties, confirming the synergistic effects of glass fibers and clays in the composites.

Yasmin *et al.* (2006) prepared the clay/epoxy nanocomposites by shear mixing method and used 1-10wt. % of clay concentration to prepare the samples. The epoxy matrix was reinforced with MMT clay particles to fabricate clay/epoxy nanocomposites. Bisphenol A was used as epoxy resin and methyl tetrahydrophthalic anhydride as the hardener. Two types of clay nanoparticles were used as the reinforcement, one was Nanomer I.28E and other was Cloisite 30B. In this

study Closite 30B showed a homogeneous dispersion of nanoparticles throughout the cross-section compared to Nanomer I.28E. As the clay content was increased, the strain to failure decreased. It was observed that the modulus of the nano-composites increased monotonically with increasing clay content. For 10wt.% of clay, the Cloisite30B/epoxy showed an increase of 53% over the neat resin, where as the other showed an increase of about 22% at room temperature. The observation further confirmed the direct relation between the degree of exfoliation and the mechanical properties of these nanocomposites. The addition of clay also found to reduce the CTE (coefficient of thermal expansion) of pure epoxy.

Avila *et al*. (2006) prepared a set of fiber glass-epoxy-nanoclay laminate composites to investigate how the plate impact strength is affected by the presence of nanoclays. The S2-glass/epoxy nanoclay composite was made a laminate with 16 layers and 65% fiber volume fraction was prepared using a vacuum assisted lay-up technique. The amount of nanoclay added into an epoxy system, in weight, was 1%, 2%, 5%, 10%, respectively. To compare the results, a set of S2-glass/epoxy laminated composites were also prepared. The addition of nanosized clays increased the composite impact strength, as the damaged area was decreased approximately 20% for small amounts of nanoclay contents. When the concentration reached around 10%; the increase on impact strength was near to 50%. Nanoclay composites showed great performance over the conventional composites under the rebound/spring effect. When the four edge clamped condition was imposed the overall composite damping was increased with the nanoclay concentration. The most favourable nanoclay concentration suggested by them was close to be 5%. This could be due to the vibration mode superposition associated to a stiffness enhancement.

Avila *et al.* (2006) investigated the influence of montmorillonite (MMT) silicate layers on glass-fiber-epoxy laminated composites behavior by low-velocity impact and X-ray diffraction tests. The nanostructure laminate prepared for the investigation was a S2-glass/epoxy-nanoclay. The nanoclay used was Nanomer I30E. The amount of nanoclay dispersed into the epoxy system, in weight, was1%, 2%, 5%, 10%, respectively. As the amount of nanoclay dispersed was increased, there was an increase in stiffness. As the stiffness reached its peak value, the fracture toughness and damping were reduced. Specimens with 5% nanoclay content showed the best performance with respect to damping. As the energy increased, the nanostructure laminate response got weaker. When the low-velocity impact results were analyzed they showed an increase on energy

absorption close to 48% for low energies, 20 J, 15% increase for medium–high energies, 60 J, and 4% for high energy, 80 J. As the amount of intercalated nanoclay content varied from 0% to 10%, the optimum condition for low-velocity impact seemed to be around at 5%.

Wetzel *et al*. (2006) analysed the characterization of epoxy nanocomposites. Special attention was directed towards reinforcing effects of nanoparticles on the polymer toughness. The incorporation of both Al_2O_3 and TiO_2 nanoparticles into the epoxy resin improved flexural stiffness, flexural strength, and fracture toughness of the polymer at the same time. Cracks in Dynamically loaded nanocomposites propagated at lower rates than in neat epoxy. The fillers were well bonded to the matrix, which was indicated by both the shift of the glass transition temperature to higher temperatures and the increase in the rubbery plateau modulus. Moreover, the presence of Al_2O_3 in epoxy increased the apparent yield stress, the yield strain, and the size of the plastic zone. Debonding effects in the process zone, as often observed in glass bead filled epoxies, were rather unlikely to participate in the toughening of EP/Al_2O_3 nanocomposites, due to the small dimensions of fillers. Further investigations would help to find relationships especially between the morphology, the relevant toughening mechanisms, and the toughness of EP/Al_2O_3 nanocomposites. It was believed that the observed property characteristics were related to the influence of nanoparticles on the molecular structure of the matrix itself.

Wang *et al.* (2006) investigated the effects of hydrothermal ageing on the thermo-mechanical properties of high performance epoxy and its nanocomposite. In this work epoxy–clay nanocomposite samples containing 2.5 wt% of clay were prepared through "slurry-compounding" approach. The cured samples were immersed in distilled water at 60°C for different periods of time before subjecting to characterization. The hydrothermal effect on the thermal/mechanical properties of neat epoxy and epoxy–clay nanocomposite was studied. The moisture uptake significantly affects the modulus at high temperature, the tensile strength, and the α-relaxation behavior. On the other hand, at low temperature, the modulus and fracture toughness were not strongly influenced. As the moisture content increased, there was a reduction in strain at break for the epoxy–clay nanocomposite while that of the neat epoxy remained constant. This effect was attributed to epoxy–clay interface debonding induced by water and formation of water cluster fillers that acted as defects in the composite.

Berketis *et al.* (2007) investigated the matrix and fiber/matrix interfacial degradation of glass fiber composites subjected to water for very long time. Laminated composite plates were manufactured by the vacuum assisted resin transfer moulding technique. The resin used was the polyester (crystic 489 PA). Durability of an isopthalic polyester resin reinforced with non-crimp glass fabrics in a hydrothermal environment for up to 30 months were examined. The weight of the composite plates initially increased due to water diffusion up to month 14 and thereafter decreased due to material losses. The initial weight increase was due to diffusion of water into the specimens. Immersion in water also resulted in significant de-bonding of the fiber/matrix interface, which allows water to penetrate the composite material by capillary action. The impacted plates were retested statically to determine residual compressive strengths for the assessment of damage tolerance. A new device was designed for the CAI tests that assured laminate failure by de-lamination propagation. The results of the CAI testing demonstrated a reduction in CAI strength, due to hydrothermal exposure for each applied level of impact loading. Immersion time of 24 and 30 months showed that a local plateau was approached in CAI strength.

Quaresimin *et al*. (2007) analysed the effect of three different commercially available nano-modifiers on the mechanical properties of an epoxy/anhydride unidirectional carbon fiber reinforced laminates. The polymeric matrix consisted of a blend of the diglycidyl ether of Bisphenol A and the epoxy novolac resin. The hardener was a hexa-hydrophthalic anhydride. The nanoclay used was Cloisite 30B. The organoclay was dispersed through a shear mixing process. Hand-layup method was used to prepare the specimens. The tensile modulus exhibited little difference between the unmodified laminates while a modest decrease was observed for the tensile strength for the VGCF (vapors grown carbon fiber) and nanoclay modified systems.

Shang-Lin *et al.* (2007) performed experimental investigation of nanocomposite coatings for healing surface flaws of glass fibers and improving alkali-resistance. He found that, with low fraction of nano-reinforcements, the nanostructures and functionalised traditional glass fibers show significantly improved both mechanical properties and environmental corrosion resistance. The most remarkable mechanical strength improvement was found for glass fibers with nanotube coatings, corresponding to the highest healing efficiency factor. No apparent strength variation appeared for nanoclay coated fiber subjected to alkaline attack, which indicated that, the

influence of moisture solvent uptake and concentration on mechanical properties decreased when the organoclay was dispersed in coating polymer. Overall, the hybrid nanocoatings caused improved fiber strength, corrosion resistance, and interfacial properties.

Chow *et al. (2007)* prepared the epoxy/glass fiber/organo-montmorillonite (OMMT) nanocomposites by hand lay-up method. In this work, the epoxy nanocomposites were characterized by X-ray diffraction (XRD), differential scanning calorimetry (DSC) and water absorption tests. Epoxy/glass fiber/OMMT hybrid nanocomposites prepared by hand-layup technique showed exfoliation characteristics and slightly enhancement in glass transition temperature. The water resistance properties of epoxy were improved by the addition of both glass fiber and OMMT, which is may be attributed to the increasing of the tortuosity path for water penetration.

Manjunatha *et al*. (2009) investigated the tensile fatigue behavior of a silica nanoparticle-modified glass fiber reinforced epoxy composite. The epoxy resin was a standard diglycidyl of Bisphenol A with an epoxide. The GFRP composite laminates were manufactured by resin infusion under flexible tooling technique. An anhydride-cured thermosetting epoxy polymer was modified by incorporating 10 wt. % of well-dispersed silica nanoparticles. The fatigue life of 10 wt. % silica nanoparticle-modified bulk epoxy was about three to four times higher than that of neat epoxy. The fatigue life of the GFRP composite with 10 wt. % silica nanoparticle modified epoxy matrix was about three to four times higher than that of the GFRP with the neat epoxy matrix. The suppressed matrix cracking and reduced crack growth rate due to the particle debonding and plastic void growth mechanisms appeared to contribute for the observed enhancement of the fatigue life in the GFRP with the nanoparticle-modified matrix.

Maitra *et al*. (2009) synthesized and evaluated PVA polymer-matrix composites reinforced with small concentrations of functionalized ND. Detailed structural characterization, employing a variety of analytical techniques, showed that the nanoparticles were distributed uniformly and did not agglomerate. Further, they appeared to interact with the polymer matrix strongly, increasing the crystallinity substantially. The mechanical properties of the PVA-ND composites were determined using nano-indentation technique. With only 0.6-wt% addition of ND, which was relatively small, significant enhancements to the hardness and Young's modulus of the PVA were observed. It was suggested that excellent adhesion between the matrix and the

functionalized ND particles was the main reason for this marked improvement in mechanical performance. These results indicated that ND could be successfully used as a filler material for making polymer composites.

Zainuddin *et al*. (2010) analysed the effect of environmental conditioning especially under hot-wet conditions on E-glass epoxy fiber reinforced composite. The weight gain was higher for all the wet conditions samples exposed to elevated temperatures. Addition of 1–2 wt% of nanoclay decreased the weight gain. Flexural properties were found to degrade with increase in time. 2 wt% GFRP composites showed enhancement in properties under all conditions over neat counterparts. In some cases, samples subjected to hot dry condition at 60^0C showed increase in properties over room temperature conditioned samples. Scanning electron micrographs provided clear evidence of the effects of nanoclay, elevated temperature and moisture absorption. Enhancement in interfacial bonding was observed in 2wt. % composite samples, both at room temperature and hot-wet conditioning.

Hossain *et al*. (2011) investigated the effect of seawater on the degradation of mechanical properties of conventional and nanophased carbon-epoxy composites. Epoxy resin was modified using 1 wt. %, 2 wt. %, and 3 wt. % nanoclay. Carbon-epoxy composites were fabricated by vacuum assisted resin transfer moulding process and compared with neat samples with and without exposure to seawater. Nanoclay was dispersed into matrix by using magnetic stirring. Mechanical characterization performed through three point bending tests showed that 2 wt. % nanoclay loading was optimum. Flexural strength and modulus were increased by 25% and 12.51%, respectively, compared to neat system for samples not exposed to seawater. Flexure samples exposed to the seawater for 30, 60, and 180-day periods revealed that samples with nanoclay retained better mechanical properties compared to neat samples. After 30-day exposure to seawater, there was no significant reduction in the strength and modulus. However, flexural strength was reduced by 10.24%, 7.08%, 5.28%, and 7.13% for neat, 1 wt.%, 2 wt.%, and 3 wt.% nanoclay-infused samples, respectively, after the samples were exposed to seawater for 180-day. At the same time flexural modulus was reduced by 12.61%, 7.16%, 4.59%, and 6.11%, respectively. From scanning electron microscopy (SEM) studies, it was found that failure occurred due to delimitation and initiated from the compression side. Nanophased composites exhibited better bonding between fiber and matrix. SEM micrographs also revealed that both

unconditioned and conditioned nanophased epoxy, which produce relatively rougher fracture surfaces compared to neat samples. Optical microscopy study revealed no significant physical change in outer surfaces of the samples conditioned up to a 90-day period.

Zafar *et al*. (2012) investigated the long term effects of moisture on the interface between a carbon fibre and an epoxy matrix. High modulus carbon fibers were used to prepare single fiber model composites based on an epoxy resin. The samples were immersed in the seawater and demineralised water and their moisture uptake behaviour was monitored. The equilibrium moisture content and diffusion coefficients for the samples were determined. DSC (Differential scanning calorimetry) had been used to analyse the moisture effects on glass transition temperature and thermal stability of the pure epoxy specimens. The results showed a reduction in the glass transition temperature (Tg) after moisture absorption. Tensile tests were also carried out for the epoxy specimens and a general decrease in the mechanical properties of the epoxy matrix was observed. Raman spectroscopy was used to observe the effects of moisture on the axial strain of the carbon fiber within the composite and stress transfer at the interface as a function of exposure time. The results show that the decrease in the mechanical and interfacial properties of the model composites under the seawater immersion is more significant than under demineralised water immersion.

CHAPTER 3 GAPS IN LITERATURE

3.1 Gaps in literature

From the literature review it was found that previous work has mainly focused on the synthesis of neat epoxy based FRP's and the characterization of the mechanical properties. There are very few publications on the hygrothermal aging studies of polymer nanocomposite FRP's. Some of the following gaps were identified in the previous research reports.

1. There are still difficulties in distributing nanoparticles homogeneously in the matrix.
2. The effect of clay addition on properties of an interply hybrid laminated nanocomposites has not been investigated.
3. With E glass fiber lamina sandwiched in between two C glass laminae, the resulting system will be more resistant to moisture ingress, have better corrosion resistance and longer useful life of resulting nanocomposites. The degradation studies conducted earlier by other researchers did not try this configuration.
4. No work reported on the hygrothermal aging studies of these nanocomposites FRP configuration.

3.2 Research problem

The present study has mainly focused upon the synthesis of epoxy layered silicate nanocomposite as matrix in fiber reinforced composites. In this study, mechanical properties and thermal stability of these FRP laminated nanocomposites has been studied. Also hygrothermal aging studies on these FRPs have been carried out.

4.1. Fabrication of specimen

4.1.1. Materials

Unidirectional E-glass fiber,C-glass fiber and M Brace a two part epoxy resin purchased from BASF Construction Chemicals (India) Private Limited. Organically modified nanoclay Closite 30B purchased from Connell Bros. Mumbai.

4.1.2. Specimen specifications

Commercially available E-glass fiber mat and chopped strand C-glass fiber had been used for making specimen. The specimen had been cut and prepared as per the assumed dimensions for tensile and bending tests respectively. The assumed dimensions of specimens are shown below:

Table 4.1 Specimen specifications for testing

Parameters for specimen	**Specimens for tensile testing**	**Specimens for Flexural testing**
Length	125 mm	125 mm
Width	15 mm	13 mm
Thickness	4 mm	4 mm

4.1.2.1. Specimen dimensions

- **For bending test**

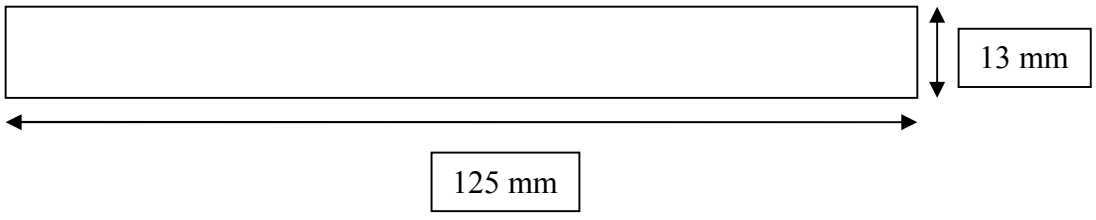

Fig.4.1 Specimen dimensions for bending test

- **For tensile test**

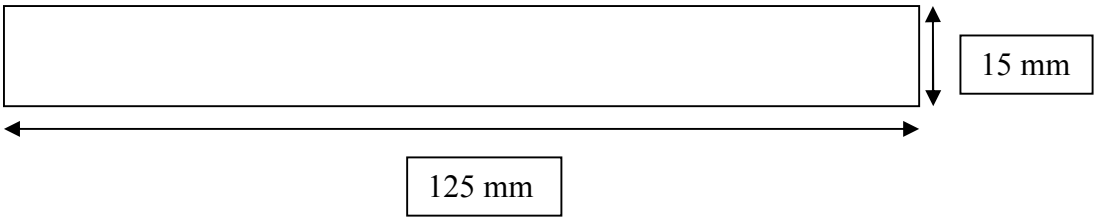

Fig.4.2 Specimen dimensions for tensile test

4.1.3. Cutting glass fiber sheet

For the experimentation, unidirectional E-glass fiber roll having 50cm width having 0^0 fiber orientation woven with polymer fibers and C-glass chopped strand fiber purchased. The sheets were initially cut a square of length 50cm.

Fig. 4.3 Uncoated E glass fiber mat used for making specimen

Fig. 4.4 Uncoated C- glass fiber mat used for making specimen

4.1.4. Mixing of nanoclay into epoxy (base):

Mechanical stirring: Epoxy base is a blue colour thick fluid. It is quite difficult to mix nano clay into it manually. So we used a mechanical stirrer and an oil bath for proper mixing of nanoclay (Fig. 4.5). Oil bath was used to heat up the epoxy to desired (60^0C) temperature for reducing the viscosity of epoxy base. Proper mechanical stirring of epoxy at this stage resulted better dispersion of clay. Different percentage of clay-.5%,2%,3% and 4% by weight were added and stirred at 60^0C for 2 hours.

Fig. 4.5 Oil bath setup with mechanical stirrer

Ultrasonication after mechanical stirring: Sonication is the act of applying sound energy to agitate particles in a sample. In the laboratory, it is usually carried out using an ultrasonic bath or an ultrasonic probe known as a sonicator. Sonication can be used to speed dissolution, by breaking intermolecular interactions. Sonication was done for evenly dispersing nanoparticles in liquids. After mechanical stirring of the epoxy solution container was placed into the ultrasonication bath for up to 2 hours.

Fig.4.6 Ultrasonication bath

4.1.5 Mixing of epoxy base solution with hardener:

After ultrasonication, the solution is mixed with the hardener in the ratio 5:2 by volume. After mixing, mechanical stirring up to 5 to 10 minutes was done. The whole procedure is shown in Fig. 4.7

Fig. 4.7 Mixing of hardener to the base component

4.1.6. Coating of nanoclay mixed epoxy to glass fiber sheets:

The mixture was then poured on to the glass fiber mat and applied uniformly using the hand layup method. For this, steel scraper was used to maintain uniformity of the solution. It was made sure that there is no air bubbles entrapped inside the epoxy applied on sheet otherwise it would create a flaw there. After applying epoxy on the both sides of first glass fiber, second fiber sheet was applied on first fiber sheet with and epoxy was applied on second fiber sheet. Finally third fiber sheet was placed on second fiber sheet and epoxy was applied on third fiber sheet. The sheet took overnight to dry. The full curing of sheet (Fig. 4.8& Fig. 4.9) was done by leaving it under ambient temperature for at least seven days before processing further.

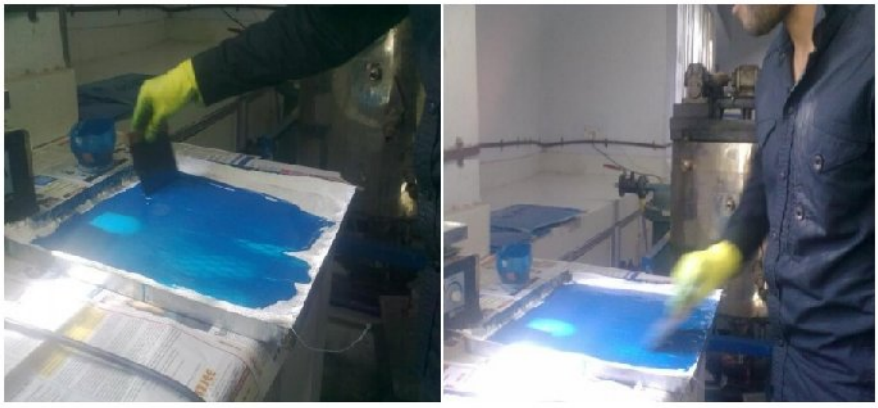

Fig. 4.8 Coating the glass fiber sheet with epoxy solution

Fig. 4.9 Coated sheets placed for curing

4.1.7. Cutting of Sheet for Samples

Once the epoxy was fully cured, cut the sheet to actual sample size using the marble cutter (Fig. 4.10).

Fig. 4.10 Marble cutter

4.2. Experimental Set-up

A set of accelerated aging tests had been carried out to evaluate performance of glass fiber reinforced polymer (GFRP) sheets embedded in epoxy matrix. The field environment very similar to that of tropical climate had been simulated. The specimens were immersed in two water baths for 30 days.

Fig. 4.11 Setup view of the water baths

The specimens were removed from the bath after an interval of 30 days. The tensile and flexural strength was measured to check the degradation in properties of composite material. Both of the water tanks were filled with water. One was of simple water and other tank was containing NaOH 5% by weight of water. Both the tanks were kept at a temperature of 45^0C.

4.2.1. Setup Fabrication:

Table 4.2 Items and quantity required

S.No.	ITEM NAME	QUANTITY
1	Water tanks	02
2	Specimens	16
3	Heating Elements	02
4	RTD Sensors	02
5	Temperature Controllers	02

4.2.2. Water tanks:

The experimental setup consists of two well insulated tanks. The tank was of cylindrical shape made out of plastic. The approximate capacity of the tank was 60 liters. Both the tanks were filled totally with tap water and set at a temperature of 45°C. NaOH was added to one tank (5% by weight of water). The water which evaporated from the tank was replenished on daily basis during experimentation. Each tank was labeled as per details of experimentation.

4.2.3. Heating element:

The setup was heated with help of commercially available heating rod elements (Fig. 4.12). Each bath was having its own heating rod connected via temperature controller (Fig.4.13). The wattage of rod was 1000KW with single phase connection. As the temperature reached the required value the power supply of rods were cut off by controllers.

Fig. 4.12 Heating element and RTD sensor in a tank

4.2.4.Temperature controller:

The objective of this set up was to maintain the bath temperature at specified value till the duration of experiment for day and night on daily basis. So a temperature controller (Fig.4.13) was connected with each of the bath along with relays cut off. The controller used the proportional-integral-derivative (PID) control to maintain the temperature. On the controller display the "Set Value" was given which was the temperature indicated in green and the "Process Value" of temperature was indicated in the red (refer Fig.4.13), which was the output from the RTD sensor. For the very first time the controller was set to auto-tune mode so that it could adjust itself according to the input variables. Once the bath had attained the set value the controller cut off its supply and after sometime it sensed the temperature if it had gone below set value, it again started heating to obtain the set value. The dimensions of the controller and actual panel used are shown in Fig.4.13 and Fig. 4.14 respectively.

Fig. 4.13 Temperature controller

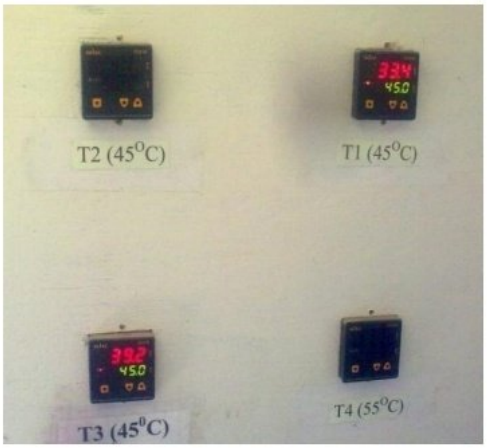

Fig. 4.14 Temperature display panel

4.3. Testing methods used in experimentation

4.3.1. Tensile testing

A Universal Tensile testing machine shown in Fig.4.15 and Fig.4.16 was used for the testing of the FRP specimen for its tensile strength. The test specimen had been prepared according to assumed dimensions. The specimen were tested until they break indicating the peak load and ultimate stress value they can bear at required time period to estimate the degradation in the same machine.

Fig. 4.15 UTM testing machine

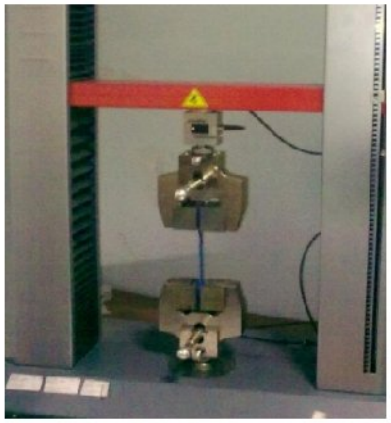

Fig. 4.16 Specimen in jaws

4.3.2. Three point flexural test

Three point bending tests of specimen were carried out in using Zwick/Roell (Fig. 4.17& Fig. 4.18).

Fig. 4.17 Three point bend test machine

Fig. 4.18 Specimen positioning

The test specimen had been prepared according to assumed dimensions. The three point bending test results can be taken as indications of strength degradation of composites after they had been hygrothermally treated.

4.3.3. Micro hardness test

Micro hardness test (shown in Fig.4.19) was conducted on specimen with different clay loadings to see the effect of clay loading on hardness values.

Fig. 4.19 Micro hardness equipment

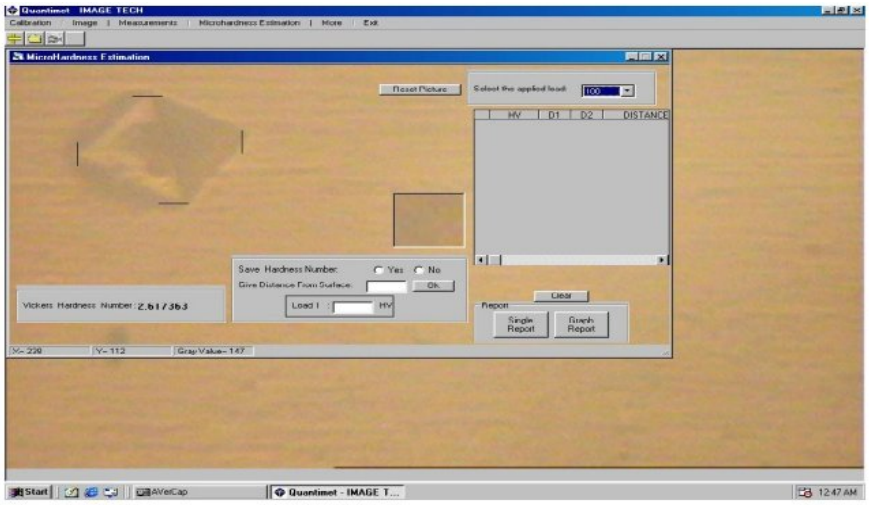

Fig. 4.20 Indent of specimen

The load applied was 50gm and VHN values were determined by applying this load by using a calibration distance of 50 units in Quantinet software as shown in Fig.4.20 used for image analyzing. The dwell time used during load application was 20 seconds. An indent is formed in diamond shape used for calculating VHN as shown in figure below.

4.3.4. X-Ray diffraction test

X-ray scattering techniques are a family of non-destructive analytical techniques which reveal information about the crystallographic structure, chemical composition, and physical properties of materials and thin films. These techniques are based on observing the scattered intensity of an X-ray beam hitting a sample as a function of incident and scattered angle, polarization, and wavelength or energy.

X-ray diffraction was used in this study to investigate the crystallographic structure of the epoxy nanocomposites. XRD will enable the changes that occur to the clay due to the intercalation and/or exfoliation of the epoxy into the clay galleries to be quantified. The d-spacing of the intergallery spacing can be determined using Bragg's Law:

$$\lambda = 2d\sin\theta$$

Where λ is the wavelength of the incidence x-ray source, d is the spacing in question, θ is ½ of 2θ the Bragg angle or the diffracted angle of the incidence x-ray beam. Below is a schematic of the previously mentioned Bragg's Law (Fig. 4.21).

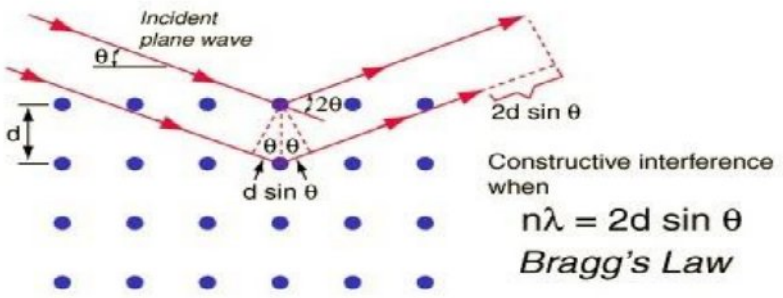

Fig. 4.21 Schematic representation of x-ray diffraction principle and the Bragg's Law

To evaluate the degree of exfoliation in the polymer, XRD measurements were carried out in a Panalytical X-ray diffractometer with Cu Kα radiation (λ=1.54Å) with a scanning speed of 10/min and at 45 kV and 40mA. During the XRD experiments, the samples were analyzed in reflection mode. All XRD scans were through 2θ of 5^0 to 15^0.

4.4. Test matrices

Table 4.3 Initial testing specimens

Specimen Name	**No. of specimens**		**Total specimens**
	Tensile	**bending**	
0 wt%	3	3	6
0.5 wt%	3	3	6
2 wt%	3	3	6
3 wt%	3	3	6
4 wt%	3	3	6
Total specimens			**30**

Table 4.4 Specimen for accelerated degradation in 45°c simple water bath

Specimen name	No. of specimens		Total specimens
	Tensile	Bending	
0 wt%	2	2	4
0.5 wt%	2	2	4
2 wt%	2	2	4
3 wt%	2	2	4
4 wt%	2	2	4
Total specimens			**20**

Table 4.5 Specimen for accelerated degradation in 45°c NaOH solution (5% by weight of water)

Specimen name	No. of specimens		Total specimens
	Tensile	bending	
0 wt%	2	2	4
0.5 wt%	2	2	4
2 wt%	2	2	4
3 wt%	2	2	4
4 wt%	2	2	4
Total specimens			**20**

5.1 MICROSCOPIC BEHAVIOUR

5.1.1 Micro-hardness

5.1.1.1 Specimen for micro hardness

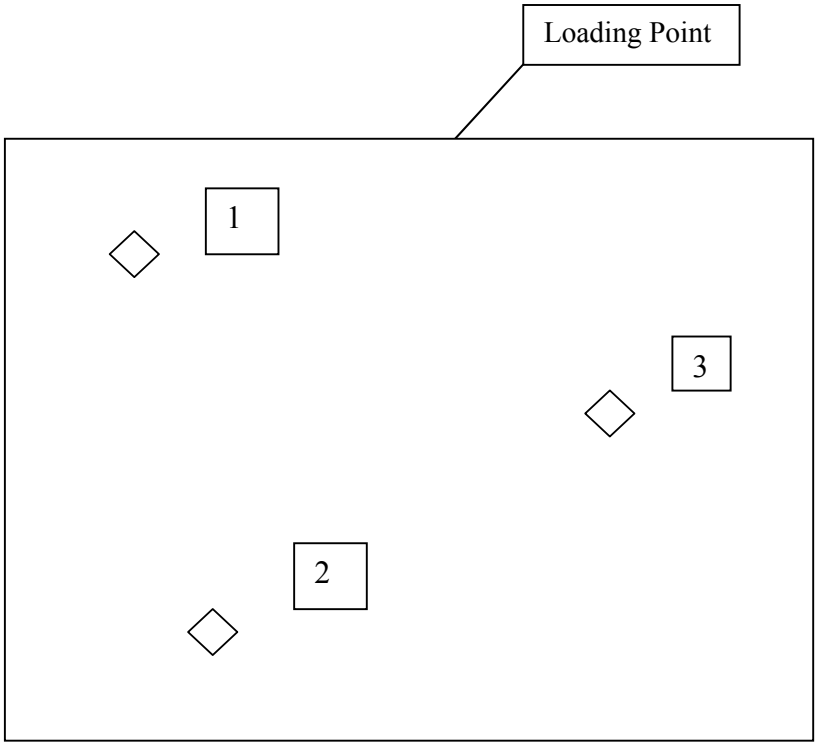

Fig. 5.1 Showing different loading points in specimen

The micro-hardness of specimen manufactured at different clay loading was measured. The table 5.1 showed the experimental observations of the nanocomposites with different nanoclay contents. An average hardness was calculated by taking measurements at 3 points in each specimen. Fig 5.2 showed the results of Vickers hardness plotted against nanoclay loading.

Table 5.1 Micro Hardness Values for Different Clay Loading Samples

Clay Loading → / Loading Points ↓	Micro hardness values				
	0 wt%	**0.5 wt%**	**2 wt%**	**3 wt%**	**4 wt%**
Point 1	4.554	6.957	7.281	5.621	5.504
Point 2	4.167	6.079	8.167	4.435	6.235
Point 3	4.203	6.079	7.157	5.789	6.032
Average	**4.308**	**6.372**	**7.535**	**5.282**	**5.927**

The maximum hardness had been measured where the nanoclay content reached 2 wt%. A decline of the hardness also appears on further increasing the nanoclay content. The hardness decreased in a significant manner from 7.535 HV (2 wt% of nanoclay) to 5.282 HV (3 wt% of nanoclay). Thus, adding a small amount of nanoclays into polymer-based materials could potentially enhance hardness of the material with the nanoclay content less than 5 wt%. However, it was also reasonable to believe that it should have an optimal limit depending on choice of constituent material and processing conditions .It was suspected that the nanoclays might retard the chemical reaction, and so cause incomplete curing process of the composites. For all specimens with high nanoclay content, the matrix might not be fully cured.

5.1.2 X-ray Diffraction Test

The X-ray Diffraction experiments were conducted on the samples having different nanoclay loading. X-ray diffractometer gives the values of d-spacing and 2θ for different samples of epoxy clay nanocomposites. An increase of the interlayer distance leads to a shift of the diffraction peak toward lower angle. The diffraction peak of Closite 30B comes out at an angle 2θ = 4.8452 having d-spacing value is d = 18.26854, Hence the shift in angle to the lower side shows the increase in d-spacing. The angle 2θ and d-spacing values of the Closite 30B and the epoxy nanocomposite having different clay loading 0.5.wt%, 2wt% , 3 wt% and 4% respectively.

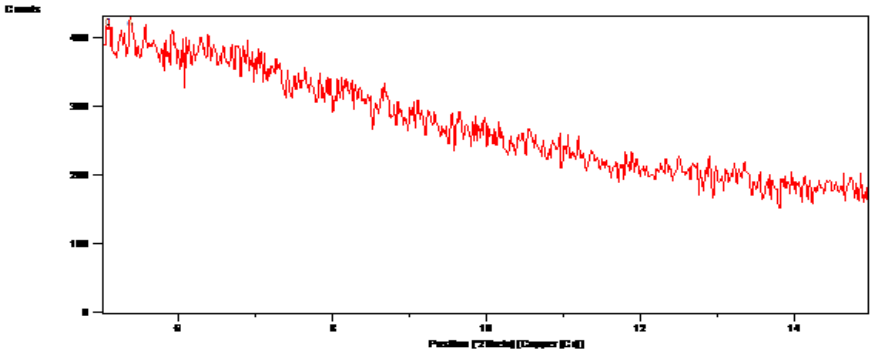

Fig. 5.2 showing XRD result of sample with 0.5% clay

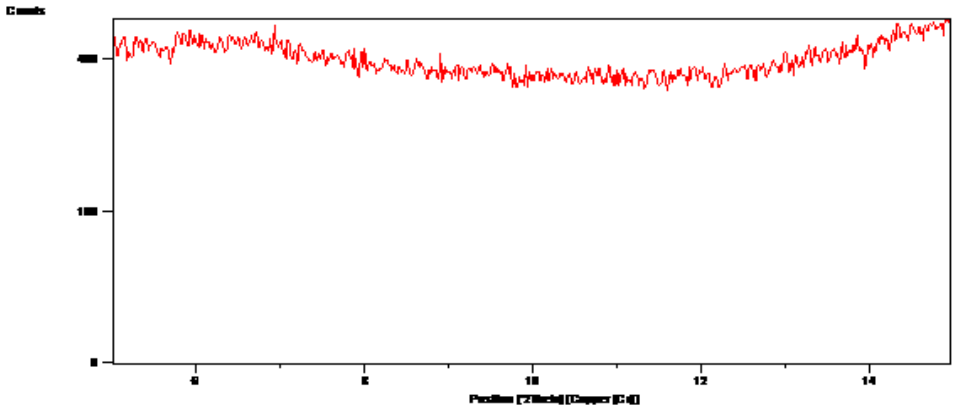

Fig. 5.3 showing XRD result of sample with 2% clay

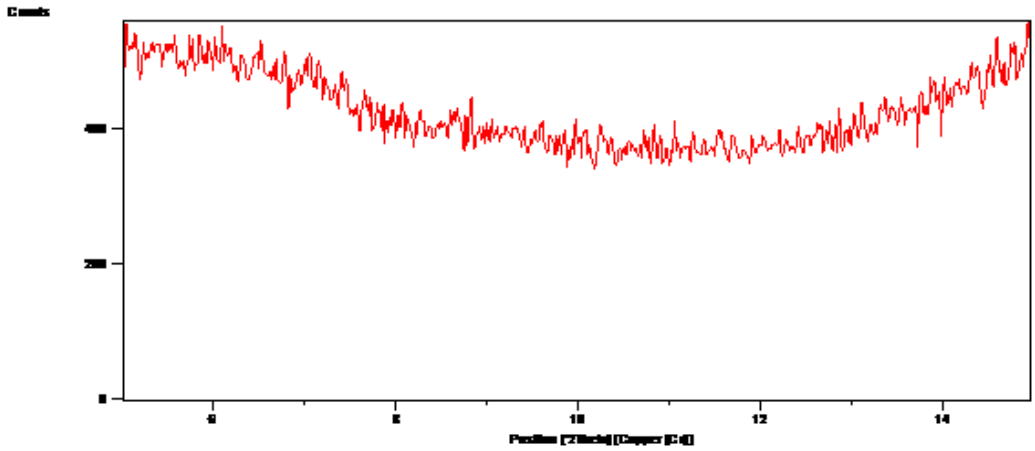

`Fig. 5.4 showing XRD result of sample with 3% clay

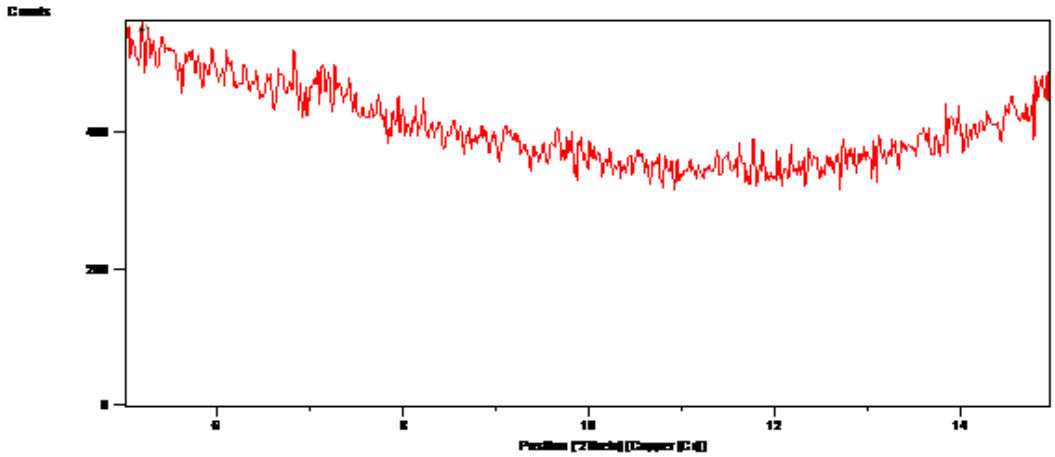

Fig. 5.5 showing XRD result of sample with 4% clay

The absence of peaks in diffraction pattern indicates formation of exfoliated nanocomposites at all levels of nanoclay loading.

5.2 Tensile Test

Table 5.2 shows the results obtained from tensile test

Table 5.2 Results of Samples from Tensile Test

Sample Name	Sample No.	Tensile Modulus (MPa)	Tensile Strength(MPa)	Strain At Tensile Strength %
0wt%	**Sample no. 1**	3680	63.5	1.20
	Sample no. 2	5060	100	1.12
0.5wt%	**Sample no. 1**	1210	95.5	1.49
	Sample no. 2	1400	81.6	1.45
2wt%	**Sample no. 1**	2320	82.6	1.40
	Sample no. 2	1880	92.1	1.22
3wt%	**Sample no. 1**	461	120	3.77
	Sample no. 2	1010	108	2.80
4wt%	**Sample no. 1**	807	101	2.79
	Sample no. 2	1480	107	2.09

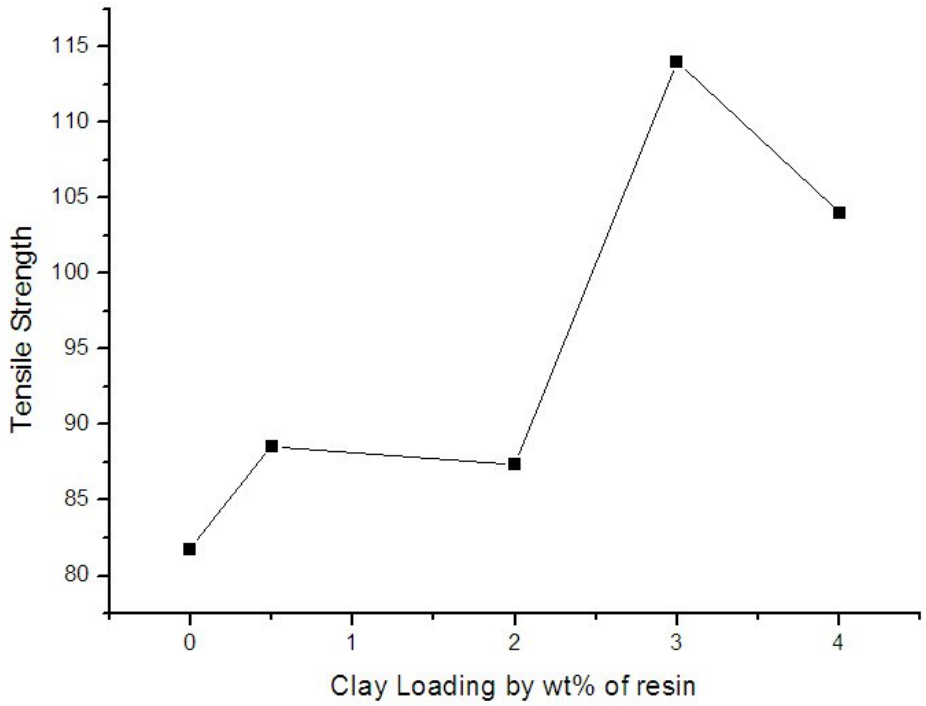

Fig. 5.6 The tensile strength of samples as a function of weight percentage of nanoclay in epoxy.

The fiber reinforced epoxy nanocomposite sample having 3wt% nanoclay loading shows the highest value of tensile stength which is 40% higher than neat epoxy glass fiber reinforced composite. The increase in the strength of the epoxy samples must be due to the introduction of nanoclay, which hindered the molecular movement of polymer chains. A significant decrease is seen in strength value at clay loading of 4wt%.The variation of ultimate tensile strength as a function of weight percentage of nanoclay in epoxy from 0wt% to 4wt% is shown in Figure 5.6.

5.3 Three-point bending test

Table 5.3 shows the results obtained from 3-point bending test

Table 5.3 Results of samples from three-point bending test

Sample Name	Sample No.	Elastic Modulus(GPa)	Flexural Strength (MPa)
0wt%	**Sample no. 1**	.817	27.3
	Sample no. 2	.858	36.5
0.5wt%	**Sample no. 1**	1.96	33.1
	Sample no. 2	1.26	35.1
2wt%	**Sample no. 1**	1.13	43.8
	Sample no. 2	.912	33.7
3wt%	**Sample no. 1**	.740	51.1
	Sample no. 2	.962	38.5
4wt%	**Sample no. 1**	1.35	43.6
	Sample no. 2	1.06	60.4

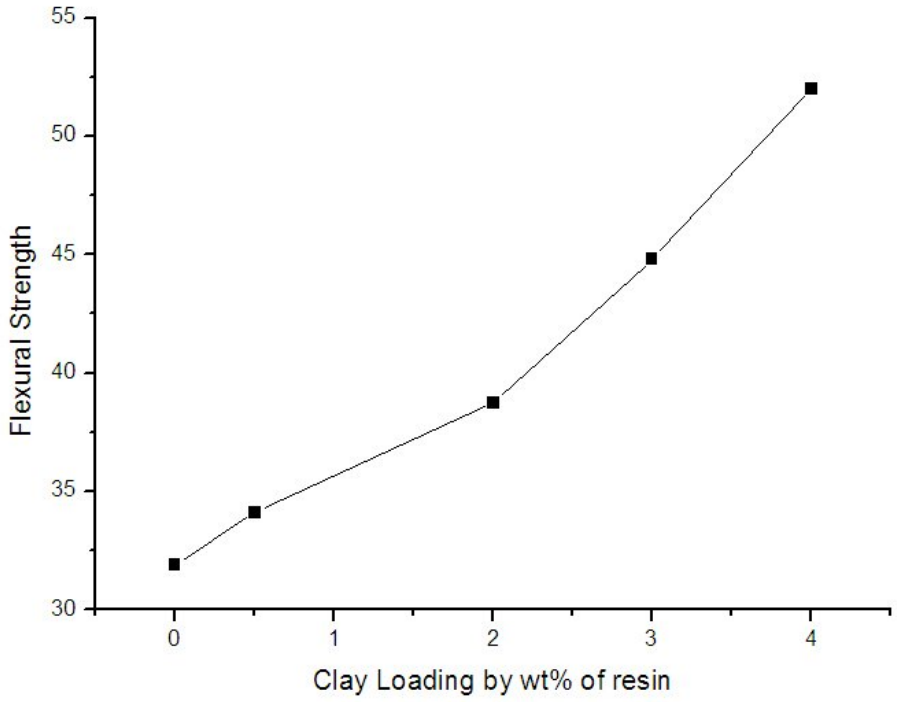

Fig. 5.7 The flexural strength of samples as a function of weight percentage of nanoclay in epoxy.

An increasing trend of flexural strength value is observed with increase in nanoclay loading upto 4wt%. A 52% improvement in strength of specimen with 4wt% clay loading is observed when compared with neat epoxy-glass composites. The flexural strength of samples against the weight percentage of nanoclay in epoxy from 0wt% to 4wt% is shown in Figure 5.7.

5.2.1 Tensile testing results of the samples simple and hygrothermally loaded

Table 5.4 Result of Degradation of Nanocomposites NaOH Tank at 45^0C using tensile test

No. of Days	Sample Name	Sample No.	Tensile Modulus (MPa)	Tensile Strength(MPa)	% Decrease in Strength
0 Day	**0wt%**	**Sample no. 1**	3680	63.5	
		Sample no. 2	5060	100	
	0.5wt%	**Sample no. 1**	1210	95.5	
		Sample no. 2	1400	81.6	
	2wt%	**Sample no. 1**	2320	82.6	
		Sample no. 2	1880	92.1	
	3wt%	**Sample no. 1**	461	120	
		Sample no. 2	1010	108	
	4wt%	**Sample no. 1**	807	101	
		Sample no. 2	1480	107	
30 Day	**0wt%**	**Sample no. 1**	1010	23.8	
		Sample no. 2	1530	9.15	79.85
	0.5wt%	**Sample no. 1**	94.1	8.48	
		Sample no. 2	826	1.15	94.57
	2wt%	**Sample no. 1**	970	19.7	
		Sample no. 2	1070	22.9	75.62
	3wt%	**Sample no. 1**	423	6.57	
		Sample no. 2	215	12.7	91.55
	4wt%	**Sample no. 1**	1100	14.2	
		Sample no. 2	645	6.63	89.88

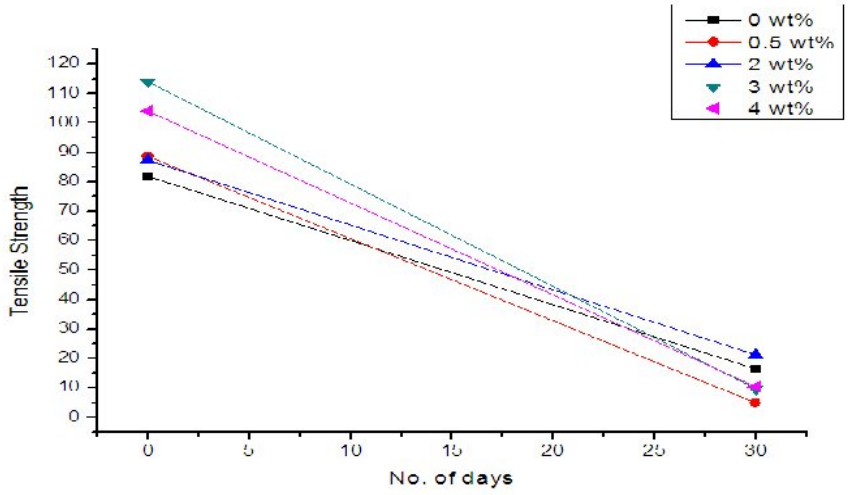

Fig 5.8 Decrease in tensile strength after degradation in NaOH

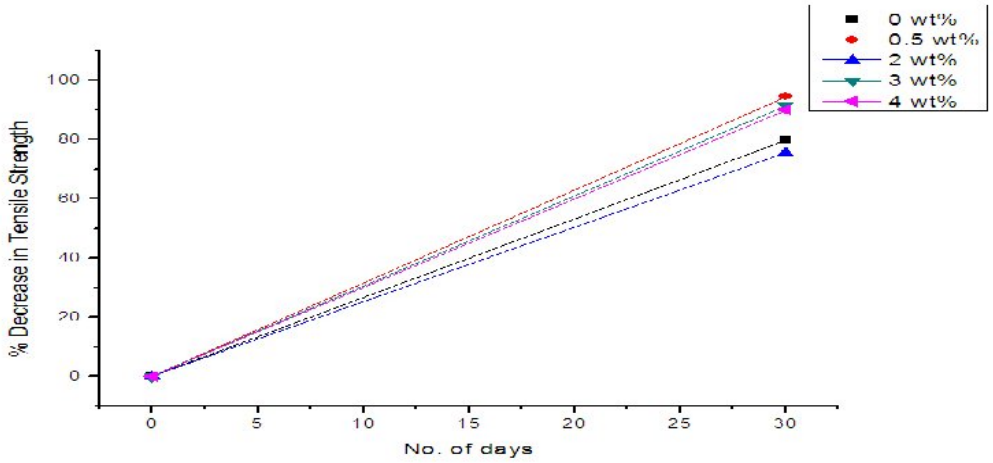

Fig 5.9 Percentage Decrease in Tensile strength after degradation in NaOH

After 30 days of water immersion of these samples, there is sharp decrease in tensile strength. The percent decrease in tensile strength value of sample having 0.5 wt% of nanoclay loading is highest among other samples when compared with samples without NaOH immersion. Figure 5.8 & 5.9 shows the effect of NaOH immersion of specimen on tensile strength. A decrease in strength of all specimens is observed.

Table 5.5 Result of degradation of nanocomposites in water tank at 45^0C using tensile test

No. of Days	Sample Name	Sample No.	Tensile Modulus (MPa)	Tensile Strength(MPa)	% Decrease in Strength
0 Day	**0wt%**	**Sample no. 1**	3680	63.5	
		Sample no. 2	5060	100	
	0.5wt%	**Sample no. 1**	1210	95.5	
		Sample no. 2	1400	81.6	
	2wt%	**Sample no. 1**	2320	82.6	
		Sample no. 2	1880	92.1	
	3wt%	**Sample no. 1**	461	120	
		Sample no. 2	1010	108	
	4wt%	**Sample no. 1**	807	101	
		Sample no. 2	1480	107	
30 Day	**0wt%**	**Sample no. 1**	599	60	
		Sample no. 2	1580	97.7	3.547
	0.5wt%	**Sample no. 1**	500	87.3	
		Sample no. 2	87.2	82.7	4.01
	2wt%	**Sample no. 1**	689	99.4	
		Sample no. 2	839	73.8	0.81
	3wt%	**Sample no. 1**	320	94	
		Sample no. 2	589	104	13.15
	4wt%	**Sample no. 1**	341	92.3	
		Sample no. 2	684	92.7	11.06

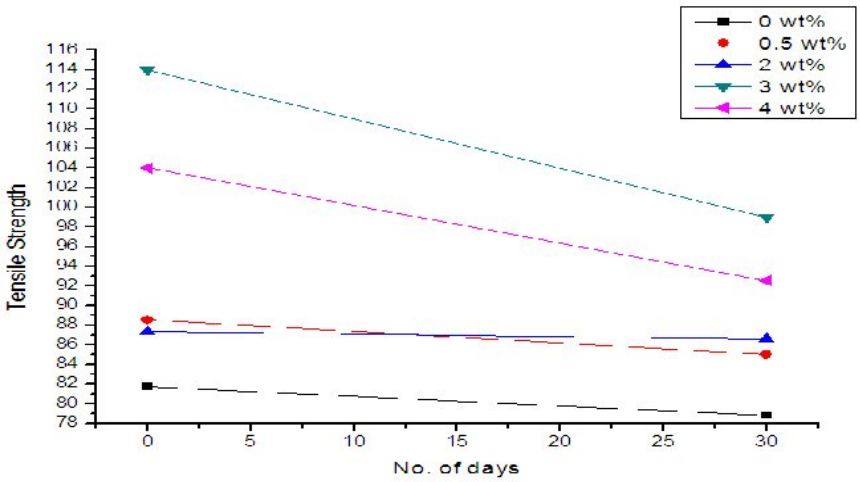

Fig 5.10 Decrease in tensile strength after degradation in water

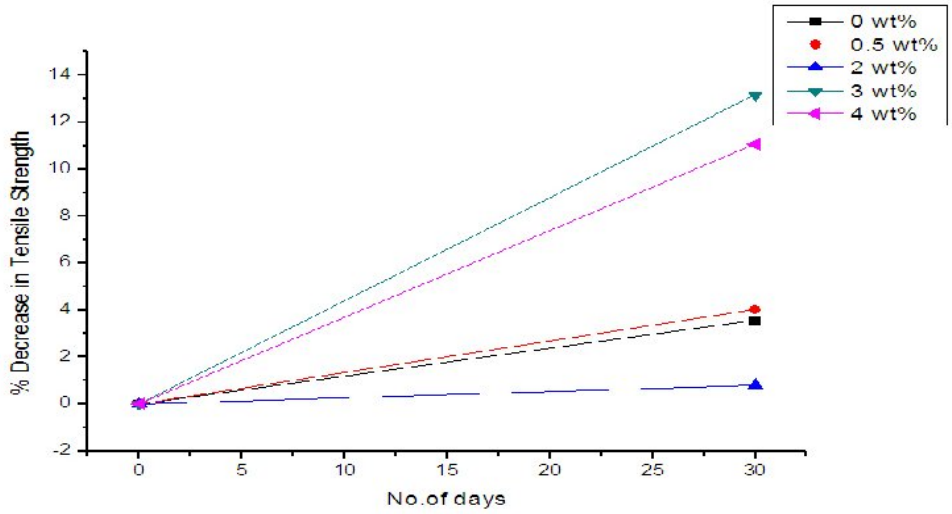

Fig 5.11 Percentage decrease in tensile strength after degradation in water

After 30 days of water immersion of these samples, there is decrease in tensile strength. The percent decrease in tensile strength value of sample having 3 wt% of nanoclay loading is highest among other samples when compared with samples without water immersion. Figure 5.10 shows the effect of water immersion of specimen on tensile strength. A decrease in strength of all specimens is observed.

5.2.2 Bending test results of nanocomposites under hygrothermal loading

Table 5.6 Results of samples for NaOH Bath at 45^0C using three-point bending test

No. of Days	Sample Name	Sample No.	Elastic Modulus (GPa)	Flexural Strength (MPa)	% Decrease in Strength
0 Day	**0wt%**	**Sample no. 1**	.817	27.3	
		Sample no. 2	.858	36.5	
	0.5wt%	**Sample no. 1**	1.96	33.1	
		Sample no. 2	1.26	35.1	
	2wt%	**Sample no. 1**	1.13	43.8	
		Sample no. 2	.912	33.7	
	3wt%	**Sample no. 1**	.740	51.1	
		Sample no. 2	.962	38.5	
	4wt%	**Sample no. 1**	1.35	43.6	
		Sample no. 2	1.06	60.4	
30 Day	**0wt%**	**Sample no. 1**	1.07	25.7	45.92
		Sample no. 2	0.753	8.8	
	0.5wt%	**Sample no. 1**	.918	12.7	45.31
		Sample no. 2	1.34	24.6	
	2wt%	**Sample no. 1**	.790	15.6	65.55
		Sample no. 2	.738	11.1	
	3wt%	**Sample no. 1**	.788	7.3	79.58
		Sample no. 2	.888	11	
	4wt%	**Sample no. 1**	1.16	10.6	75.76
		Sample no. 2	1.25	14.6	

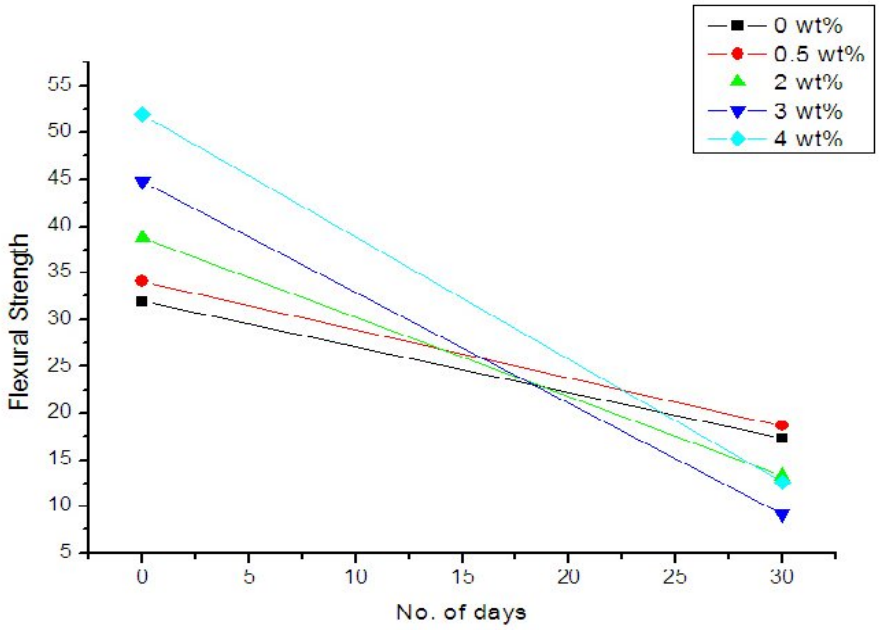

Fig 5.12 Decrease in flexural strength after degradation in NaOH

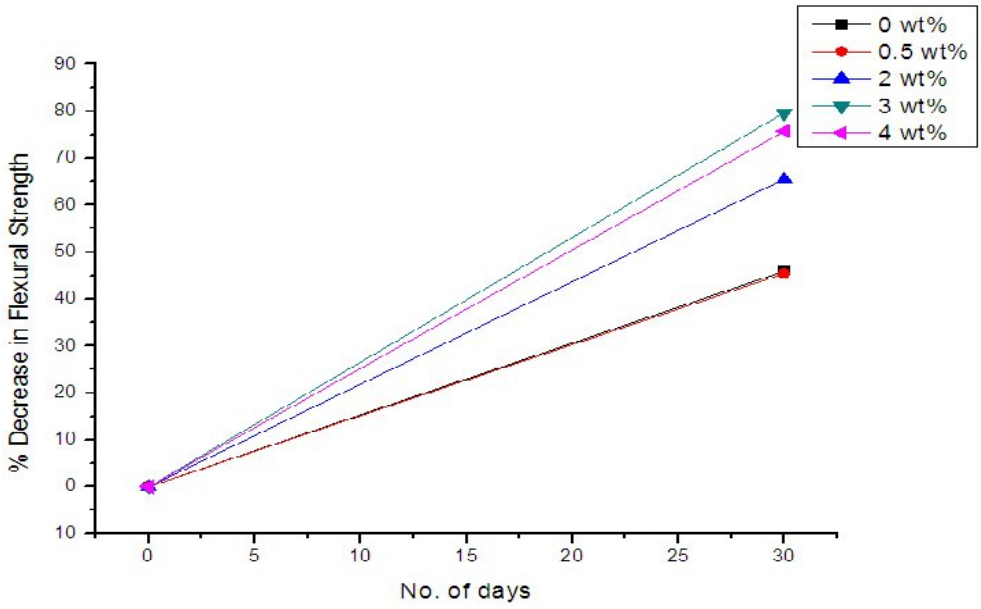

Fig 5.13 Percentage decrease in flexural strength after degradation in NaOH

Table 5.7 Results of Samples from WATER Bath at 45^0C using three-point test

No. of Days	Sample Name	Sample No.	Elastic Modulus (GPa)	Flexural Strength (MPa)	% Decrease in Strength
0 Day	**0wt%**	**Sample no. 1**	.817	27.3	
		Sample no. 2	.858	36.5	
	0.5wt%	**Sample no. 1**	1.96	33.1	
		Sample no. 2	1.26	35.1	
	2wt%	**Sample no. 1**	1.13	43.8	
		Sample no. 2	.912	33.7	
	3wt%	**Sample no. 1**	.740	51.1	
		Sample no. 2	.962	38.5	
	4wt%	**Sample no. 1**	1.35	43.6	
		Sample no. 2	1.06	60.4	
30 Day	**0wt%**	**Sample no. 1**	.678	25	
		Sample no. 2	.854	32	10.65
	0.5wt%	**Sample no. 1**	1.14	31.8	
		Sample no. 2	1.01	31.6	7.04
	2wt%	**Sample no. 1**	.596	41.2	
		Sample no. 2	1.22	33.4	4.25
	3wt%	**Sample no. 1**	1.01	44.5	
		Sample no. 2	1.01	37.2	8.82
	4wt%	**Sample no. 1**	1.18	43.3	
		Sample no. 2	1.45	47.9	12.30

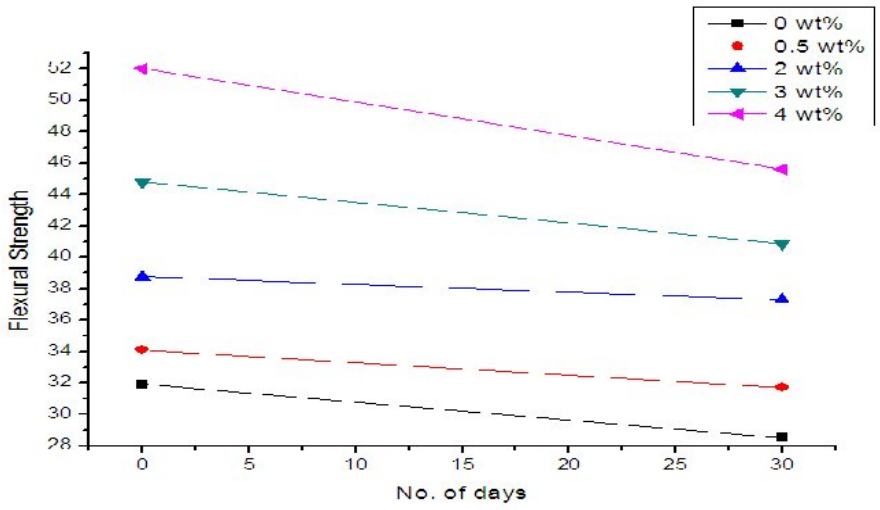

Fig 5.14 Decrease in flexural strength after degradation in water

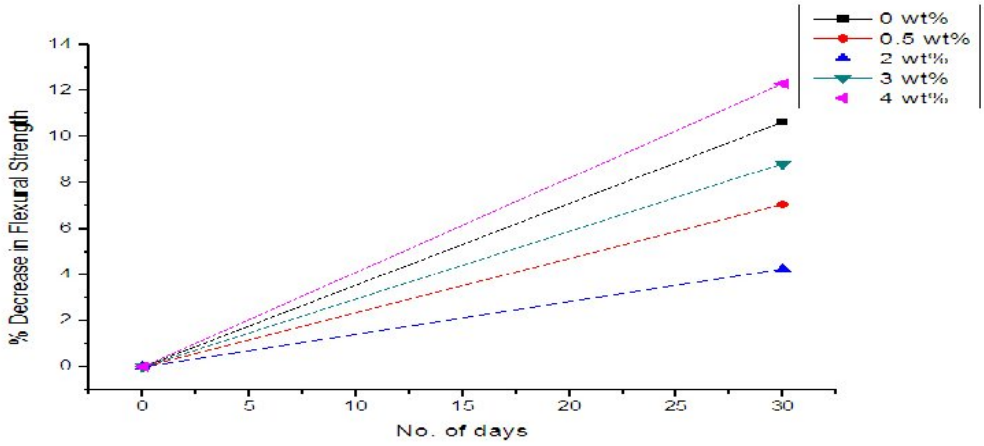

Fig 5.15 Percentage decrease in flexural strength after degradation in water

From tables 5.7 and 5.8, the NaOH immersion of 3 wt% specimen results in 79.58% decrease in flexural strength but the water immersion of 3 wt% specimen results in 8.8% decrease in flexural strength which shows that there is tremendous decrease in flexural strength of samples immersed in NaOH as compared to samples immersed in water.

CHAPTER 6 CONCLUSION AND FUTURE SCOPE

6.1 Conclusion

Epoxy modified with Closite 30B® has been used for preparing an interply hybrid laminated nanocomposites. In these nanocomposites unidirectional E-glass fiber was sandwiched between chopped strand C-glass fiber. Five different nanoclay-epoxy compositions (0.5 wt%, 2 wt%, 3 wt% and 4 wt %) were prepared in order to show the variation in mechanical property and thermal stability. Two different areas of characterization instruments were employed to study the mechanical and microstructural behaviors of the nanoclay-epoxy samples. For bending test and tensile test a Zwick/Roell universal testing machine was used and for micro hardness Vickers' hardness tester was used, the ultimate tensile strength, flexural strength and Vickers' hardness values were obtained. From the microstructural analysis instruments such as X-Ray Diffractometry (XRD), the positions of the diffraction peaks of the samples were obtained.

From the Vickers' hardness results of the nanoclay-epoxy samples, the 2wt% nanoclay sample was the hardest among all the compositions with the largest HV value of 7.535. Compared with that of pure epoxy sample of HV 4.308, the increment is 43% in Vickers' hardness value. And 3wt% nanoclay sample showed a drop in the hardness with value of HV 5.282. This might be attributed possible aggregation of nanofiller clay at some sites. From the XRD results, the absence of peaks in diffraction pattern indicates formation of exfoliated nanocomposites at all levels of nanoclay loading. From the tensile results, 3wt% nanoclay loading specimen showed the highest value of tensile strength which is 40 % higher than neat epoxy glass fiber reinforced composite. The increase in the strength of the epoxy samples must be due to the introduction of nanoclay, which shares the stress imposed on the polymer chains. The individual platelets have much higher mechanical properties as compared to polymer matrix. From the flexural results, when compared with neat epoxy-glass composites 52% improvement in strength of specimen with 4wt% clay loading was observed.

The durability at 45^0C studies were conducted on nanocomposites by exposing to water and NaOH for a period of 30 days then evaluating the mechanical property degradations. Mechanical properties were found to degrade with increase in time. The properties degradation in NaOH environment was more severe as compared to simple water.

6.2 Future scope

1. To see the effect of nanoclay on FRP`s, experiments can be repeated by changing the types of glass fiber.
2. The experiments can be performed on polyester as matrix system, since with this matrix the barrier properties of composites can be enhanced.
3. For chemical resistance study, base can be changed.
4. The duration of current experiments can be increased to see the effect in long term.
5. Epoxy of different structure& properties can be used

REFERENCES

1. **Alexandre M,** (2000), Polymer-layered Silicate Nanocomposites: Preparation, Properties and uses of a New Class of Materials, Mater. Sci. Eng. Rep., 28, 1-63.
2. **Avila A, Almir S and Marcelo I.,** (2006), A study on nanostructured plates behaviour under low-velocity impact loading. Material and design, 34, 28-41.
3. **Avila A, Horacio V. and Marcelo I.,** (2005), The nanoclay influence on impact response of laminated plates, Latin American journal of solids and structures, 3, 3-20.
4. **Berketis K, Tzetzis D and Hogg P.J,** (2007), The influence of long term water immersion ageing on impact damage behaviour and residual compression strength of glass fiber reinforced polymer (GFRP), Material and design, 29, 1300-1310.
5. **Biron, M.,** (1973), Thermosets and Composites-Technical Information for Plastics Users, New York: Elsevier.
6. **Chow W, Bakar A and Ishak Mohamad A.,** (2005), Water absorption and hygrothermal aging study on organomontomorrillonite reinforced polyamide6/polypropylene nanocomposites, Journal of applied polymer science, vol 98, 780-790.
7. **Gao Shang-Lin, Mader E and Plonka R.,** (2007), Nanocomposite coating for healing surface defects of glass fiber and improving interfacial adhesion, Composite science and technology, 68, 2892-2901.
8. **Hossain M. K., Imran K. A., Hosur M. V. and Jeelani S.,** (2011), Degradation of Mechanical properties of convectional and nanophased Carbon/Epoxy composites in seawater.
9. **Jena P,** (1996), Nanostructured materials**,** Nova Science New York.
10. **Kornmann X, Rees M, Thomsan Y, Necola A, Barbezat M and Thomsan R,** (2005), Epoxy layered silicate nanocomposite as matrix in glass fiber-reinforced composites, Composite science and technology, 65, 2259-2268.
11. **Lei Wang, Ke Wang, Ling Chen and Chaobin He,** (2006), Hydrothermal Effects on the Thermo-mechanical Properties of High Performance Epoxy/Clay Nanocomposites, Polymer engineering science, 46, 215–221.

12. **Lin Li-Yu, Lee Joong-Hee, Hong Chang-Eui, Yoo Gye-Hyoung, Advani Suresh G,** (2005), Preparation and characterization of layered silicate/glass fiber/epoxy hybrid nanocomposites via vacuum-assisted resin transfer moulding (VARTM), Composites Science and Technology 66 (2006) 2116–2125.
13. **Lowenstein, K. L.** (1973), Manufacturing Technology of Continuous Glass Fibers, New York: Elsevier.
14. **Manjunatha C.M, Taylor A.C, Kinloch A.J and Sprenger S,** (2009), The tensile fatigue behavior of a silica nanoparticle-modified glass fiber reinforced epoxy composites, Composite science and technology, 70, 193-199.
15. **Njuguna J and Pielichowski K,** (2003),Advanced Engineering Materials, 5, 769.
16. **Quaresimin M. and Varley R. J,** (2007). Understanding the effect of nano-modifier addition upon the properties of fiber reinforced laminates, Composite science and technology, 68, 718-726.
17. **Rumiana K,** (1994), Thermoset Nanocomposites for Engineering Applications.
18. **Sakaki H and Noge H., eds,** (1994), Springer Verlag, Berlin.
19. **Sinha R. S., Okamoto M.,** (2003), Polymer/layered silicate nanocomposites: a review from preparation to processing, Prog. Polym. Sci., 28, 1539–1641.
20. **Wang H, Zeng C, Elkovitch M and Koelling W. K,** (2001), Processing and properties of polymeric nanocomposites, Polymer engineering and science, 41, 11.
21. **Wetzel B, Rosso P, Haupert F and Friedrich K,** (2006), Epoxy nanocomposite-fracture and toughening mechanisms, Engineering fracture mechanics, 73, 2375-2398.
22. **Yasmin A, Luo J.J, Abot J.L, Danial I.M,** (2006), Mechanical and thermal behavior of clay/epoxy nanocomposites, Composite science and technology, 66, 2415-2422.
23. **Zafar A, Bertocco F, Schjodt-Thomsen J and Rauhe J.C**, (2012), Investigation of the long term effects of moisture on carbon fibre and epoxy matrix composites, Composite science and technology.
24. **Zainuddin S, Hosur M.V, Zhou Y, Kumar Ashok and Jeelani S,** (2010), Durability study of neat/nanophased GFRP composite subjected to different environmental conditioning, Material science and engineering, A 57, 3091-3099.